AMERICAN SOCIETY FOR MICROBIOLOGY | Antimicrobial Agents and Chemotherapy

A mechanism-based pharmacokinetic/pharmacodynamic analysis of polymyxin B-based combination therapy against carbapenem-resistant *Klebsiella pneumoniae* isolates with diverse phenotypic and genotypic resistance mechanisms

Ramya Mahadevan,[1] Estefany Garcia,[2] Rajnikant Sharma,[1] Hongqiang Qiu,[2,3,4] Ahmed Elsheikh,[2] Robert Parambi,[2] Cely Saad Abboud,[5] Fernando Pasteran,[6] Maria Soledad Ramirez,[7] Keith S. Kaye,[8] Robert A. Bonomo,[9,10,11,12,13] Gauri G. Rao[1,2]

AUTHOR AFFILIATIONS See affiliation list on p. 15.

ABSTRACT Increased resistance to β-lactams/β-lactamase inhibitors by mutations in β-lactamase genes, porins, and efflux pumps complicates the management of carbapenem-resistant *Klebsiella pneumoniae* (CRKP). Polymyxin B (PMB)-based combination therapy is the best alternative treatment for middle and low-income countries that cannot access the latest medicines. It is crucial to know both phenotypic and genotypic characteristics of a pathogen to understand the killing effect of each drug and its combinations. Hence, our objective was to incorporate mechanistic insights gained from resistance mechanisms of each isolate to develop a mechanism-based pharmacokinetic/pharmacodynamic model. Six clinical CRKP isolates with diverse genotypic resistance expressing bla_{KPC}, bla_{NDM}, porin, and mgrB mutations were used for static concentration time kill (SCTK) assays to evaluate the rate and extent of killing by monotherapy, double and triple combinations using PMB (0.5–64 mg/L), meropenem (10–120 mg/L), and fosfomycin (75–500 mg/L). Isolate BRKP28 expressed non-functional MgrB (a regulatory protein) and high-level phenotypic resistance (PMB MIC: >128 mg/L). In line with the observed resistance, the model estimated that BRKP28 had a reduced maximum killing rate constant for PMB (3.61 h^{-1}) relative to other isolates. The mechanistic synergy of PMB, due to outer membrane disruption, was incorporated into three isolates with porin mutations. PMB demonstrated 83%–88% mechanistic synergy with meropenem and 81%–98% with fosfomycin. The model further estimated that a very low concentration of PMB (0.49–0.64 mg/L) was sufficient to achieve 50% of the maximum synergy. Simulations using population pharmacokinetic models showed that combination therapy of PMB (1 mg/kg q12h) and fosfomycin (8 g q8h) achieved >73% reduction in area under the bacterial load-versus-time curve across four isolates. The triple combination therapy achieved a 67.7% reduction in non-carbapenamase producing isolate. These findings demonstrates that a low PMB dosing regimen (1 mg/kg q12h) can produce synergistic effects in combination therapy and may be effective in managing infections caused by CRKP, including PMB resistant isolates.

KEYWORDS carbapenem resistant *Klebsiella pneumoniae*, mechanism based PK/PD model, polymyxin B based combination therapy

Infections caused by carbapenem-resistant Enterobacterales (CRE) are a significant public health crisis, as the development of new antibiotics is not keeping pace with the rapid rise in antimicrobial resistance (AMR). The global incidence of CRE has doubled in just two years, from an average of 4.2% in 2018 to 8.04% between 2020 and 2022 (1). In the United States, 83% of clinical CRE isolates are carbapenemase-producing, with

Editor James E. Leggett, Providence Portland Medical Center, Portland, Oregon, USA

Address correspondence to Gauri G. Rao, gaurirao@usc.edu.

Ramya Mahadevan and Estefany Garcia contributed equally to this article. Author order was determined by mutual agreement.

The authors declare no conflict of interest.

Received 20 May 2025
Accepted 17 October 2025
Published 19 December 2025

the most prevalent β-lactamase (*bla*) genotypes being bla_{KPC} (80%), followed by bla_{NDM} (15%), bla_{OXA-48} (7%), and bla_{IMP} (5%). Between 2019 and 2021, bla_{KPC} prevalence decreased 1.3-fold, while isolates carrying other resistance genes increased by 5- to 8-fold. Non-carbapenamase-producing CRE isolates typically exhibit resistance through other mechanisms, including extended-spectrum β-lactamases (ESBLs), disruptions in outer membrane porin, and/or overexpression of genes encoding efflux pumps (2).

A comprehensive meta-analysis has demonstrated that integrating rapid molecular diagnostics (RMDs) to identify pathogens responsible for bloodstream infections with antimicrobial stewardship programs significantly lowers mortality rates, reduces the time to effective therapy, and shortens hospital stays (3). Recent studies, PRIMERS I and II (Platforms for Rapid Identification of MDR-Gram negative bacteria and Evaluation of Resistance Studies), have evaluated the accuracy of RMD platforms in identifying *bla* genotypes, which confer β-lactam resistance, to assist in the appropriate selection of β-lactams (4). Collectively, these studies underscore the importance of RMDs in the global effort to combat AMR.

The recent approval of novel β-lactamase inhibitors including avibactam, relebactam, vaborbactam, taniborbactam, and enmetazobactam has significantly advanced efforts to reduce CRE-related infections (5, 6). Additional inhibitors including ledaborbactam, zidebactam, xeruborbactam, funobactam, and nacubactam are in late-stage development or nearing approval (7). However, resistance to β-lactam/β-lactamase inhibitors has already been observed (8). Key resistance mechanisms include mutations in bla_{KPC}, changes in outer membrane permeability, and the presence of bla_{NDM} (2).

The diversity of resistant mechanisms in CRE makes it challenging to identify appropriate therapies that are effective in managing CRE infections. In the absence of new antimicrobial agents, optimizing the use of existing antibiotics is a crucial strategy to combat AMR (9). A multi-study analysis of patients infected with carbapenem-resistant *Klebsiella pneumoniae* (CRKP) found that combination therapy reduced mortality rates to 25%–31%, a 2- to 2.35-fold improvement over monotherapy with mortality rates of 50%–73% (10–12). Current polymyxin guidelines recommend polymyxin B-based combinations as an effective alternative for CRE infections, though their nephrotoxicity limits widespread use (13). Recent clinical trials, including OVERCOME and AIDA, have shown reduced mortality with colistin-meropenem combination therapy compared to monotherapy (14, 15).

Despite recent advancements, clinicians continue to face challenges in selecting the most appropriate antibiotic combinations for CRE infections. Fosfomycin, a bactericidal drug with a favorable safety profile and a distinct mechanism of action (inhibiting the peptidoglycan synthesis at an earlier stage) than β-lactams, has emerged as a promising candidate for combination therapy against Gram negative pathogens. Notably, fosfomycin has demonstrated *in vitro* and *in vivo* synergy with both meropenem and polymyxin B, and this synergy appears unaffected by polymyxin resistance-associated mutations (*mgrB*, *crrB*, *pmrA*, *pmrB*, *pmrC*) or the presence of β-lactamases (16).

Given that an antibiotic's spectrum of activity is shaped by the underlying resistance mechanism (carbapenemase producing CRKP vs non-carbapenamase producing CRKP), a systematic and rational approach that integrates resistance mechanisms and susceptibility data is necessary for effective management of CRE infections.

To this end, static concentration time-kill assays were performed to evaluate the impact of treatment with polymyxin B, meropenem, and fosfomycin as monotherapies, as well as polymyxin B-based combinations with either fosfomycin or meropenem, and a triple combination of all three drugs against six CRKP clinical isolates representing both carbapenamase producing and non-carbapenamase producing clinical isolates. The strains were genomically characterized to elucidate mechanistic insights into their killing activity based on the resistance mechanisms expressed. The objective of this study was to characterize the bacterial killing dynamics of six CRKP isolates by integrating their phenotypic and genotypic resistance profiles to inform the development of a mechanism-based pharmacokinetic/pharmacodynamic (PK/PD) model (MBM).

RESULTS

Susceptibility and resistance gene profiles for clinical isolates

The minimum inhibitory concentrations (MICs) and relevant resistance genes for the six isolates are summarized in Table 1. Among the six isolates, four isolates (BRKP61, BRKP67, BRKP76, BRKP28) expressed bla_{KPC-2} with outer membrane porin mutations. BRKP67 and BRKP28 also exhibited non-functional MgrB protein, conferring resistance to polymyxin B. The non-carbapenemase producer, KP0016-1 harbored outer membrane porin mutations, while KP0052-1, expresses bla_{NDM} without porin mutations. The complete gene characterization profiles for each isolate are provided in Table S2.

Evaluation of pharmacodynamic effect with mono and combination therapy

Figure 1A summarizes the percentage of bactericidal activity and extent of reduction in bacterial burden over time (i.e., the area under the bacterial load-versus-time curve, AUC_CFU) achieved with each polymyxin B-based double and triple combinations. Bactericidal activity increased progressively from 33% with polymyxin B-meropenem, to 67% with polymyxin B-fosfomycin, and 83% with the triple combination. Increasing polymyxin B concentration from 2 to 4 mg/L enhanced bactericidal activity across all strains, in combination with meropenem (PMB-MEM: 0% to 33%), fosfomycin (PMB-FOF: 33% to 67%) and the triple combination (PMB-MEM-FOF: 67% to 83%). Overall, the triple combination showed greater bacterial reduction than double combinations, as reflected by lower AUC_CFU value of 33.8 $\log_{10}$ CFU·h/mL. The bacterial reduction was comparable between the higher concentration double combination (PMB 4 mg/L + FOF 150 mg/L) and the lower concentration triple combination (PMB 2 mg/L + MEM 40 mg/L + FOF 75 mg/L), with similar median AUC_CFU (range: 32.5–37.2 $\log_{10}$ CFU·h/mL).

Polymyxin B-based combinations were effective against isolates expressing carbapenemases and porin mutations (Fig. 1C and D). Enhanced pharmacodynamic activity was observed with polymyxin B combination therapy against KP0016-1 despite the absence of functional porins. In polymyxin B-resistant isolates, double combinations resulted in substantial bacterial reduction against BRKP67 but minimal activity against BRKP28 (Fig. 1B). The triple combination with higher polymyxin B concentrations (PMB 4 mg/L + MEM 40 mg/L + FOF 75 mg/L), yielded comparable bacterial reduction for both BRKP67 and BRKP28 (40.1 vs 50.3 $\log_{10}$ CFU·h/mL).

Mechanism-based PK/PD model

The mechanism-based PK/PD model structure shown in Fig. 2 describes the time-kill dynamics for six isolates, incorporating both subpopulation synergy (where polymyxin B targets bacterial populations resistant to meropenem and/or fosfomycin, and vice versa) and mechanistic synergy. Among the polymyxin B resistant isolates, BRKP28 (harboring a non-functional MgrB protein and polymyxin B MIC >128 mg/L) exhibited the lowest maximum killing rate constant for polymyxin B ($Kmax_{PMB}$ = 3.61 h^{-1}) compared with other isolates (6.61–13.42 h^{-1}). Interestingly, BRKP67 which also carried an *mgrB*

TABLE 1 Antimicrobial resistance genes and MICs for each of the six CRKP isolates[a]

Isolate	Resistance genes					PMB MIC (mg/L)	FOF MIC (mg/L)	MEM MIC (mg/L)
	Carbapenamase	*mgrB*	*ompK35*	*ompK36*	*ompK37*			
BRKP28	bla_{KPC-2}	NF	NF	NF	Present	>128 R	128 R	256 R
BRKP61	bla_{KPC-2}	F	NF	NF	Present	<0.5 I	256 R	128 R
BRKP67	bla_{KPC-2}	NF	NF	NF	Present	8 R	32 R	64 R
BRKP76	bla_{KPC-2}	F	NF	NF	NF	<0.5 I	32 R	64 R
KP0016-1	Not present	F	NF	NF	NF	<0.5 I	64 R	64 R
KP0052-1	bla_{NDM-4}	F	Present	Present	Present	<0.5 I	64 R	64 R

[a]NF, non-functional; F, functional, Polymyxin B and meropenem MICs were interpreted using CLSI breakpoints for *Klebsiella pneumoniae*. Fosfomycin MICs were interpreted using EUCAST breakpoint for *E. coli*. I, intermediate, R, resistant.

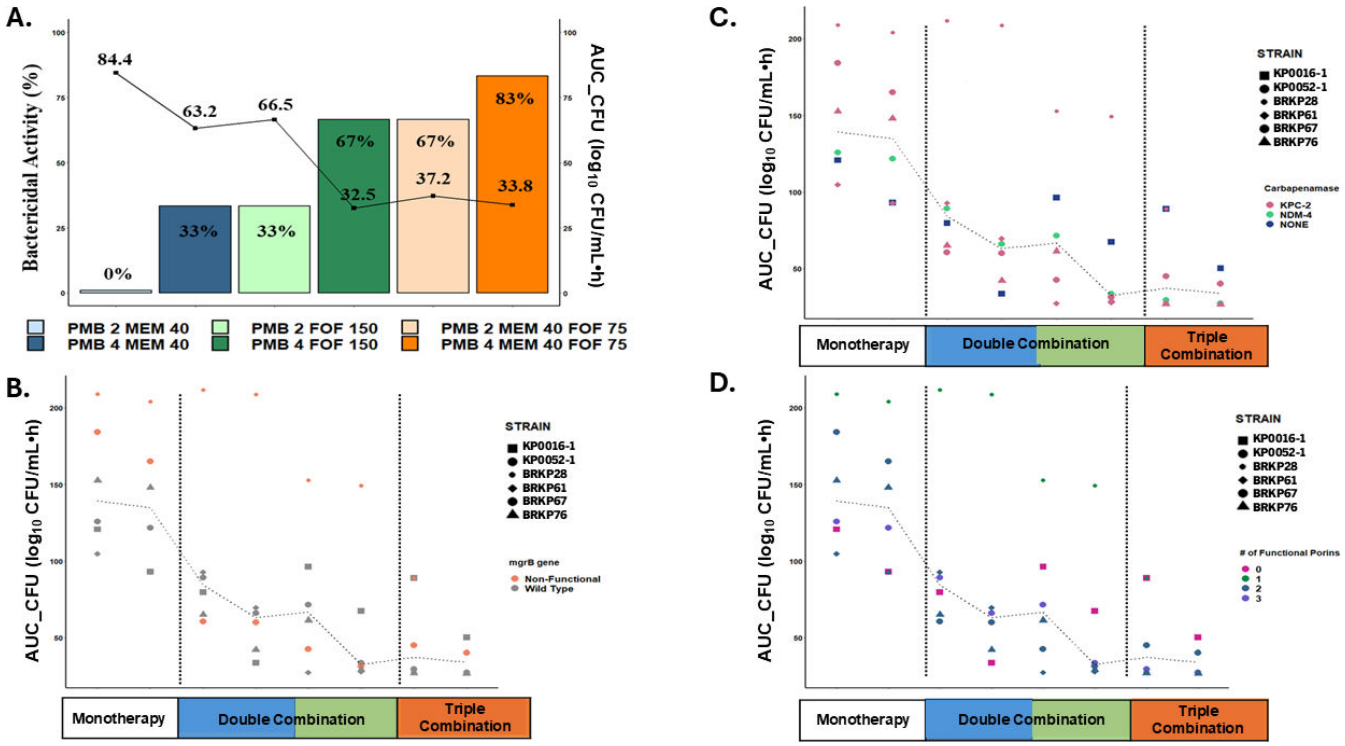

FIG 1 (A) illustrates the bactericidal activity and extent of bacterial reduction (AUC_CFU) for polymyxin B-based double and triple combinations. The bar graph represents the percentage of bactericidal activity, while the line graph shows the median AUC_CFU achieved by each drug regimen. (B–D) show the corresponding AUC_CFU for each of the six CRKP isolates, categorized by their respective resistance mechanisms: *mgrB* protein (B), carbapenemase production (C) and the number of functional porins (D).

mutation but had a lower polymyxin B MIC (8 mg/L), showed a slightly higher $Kmax_{PMB}$ of 9.08h^{-1}. Despite similar resistance mutations, the reduced killing effect of polymyxin B against BRKP28 may be due to additional uncharacterized resistance mechanisms.

The non-carbapenemase-producing isolate KP0016-1, carrying three porin mutations, showed the lowest killing rate constant for both meropenem (1.56 h^{-1}) and fosfomycin (0.64h^{-1}). Among isolates with a similar meropenem MICs of 64 mg/L, the bla_{NDM-4} producer displayed a lower *Kmax* for meropenem (3.05 h^{-1}) than bla_{KPC-2} producers (4.16–5.41h^{-1}). Furthermore, BRKP61 (MIC: 128 mg/L) and BRKP28 (MIC: 256 mg/L), both bla_{KPC-2} producers with higher meropenem MICs demonstrated correspondingly lower *Kmax* values for meropenem (2.13 h^{-1} and 3.70h^{-1}, respectively).

BRKP61, KP0016-1, and BRKP76 isolates carried porin mutations, which are assumed to reduce the penetration of hydrophilic drug molecules such as meropenem and fosfomycin. The mechanistic synergy of polymyxin B, through outer membrane disruption, was expected to enhance the target site exposure of both drugs in these isolates. For meropenem, the mechanistic synergy with polymyxin B resulted in $Imax_{,M,PMB}$ values of 0.84, 0.83, and 0.88 for BRKP61, BRKP76, and KP0016-1, respectively, with IC50 values (polymyxin B concentration required to achieve 50% of $Imax_{,M,PMB}$) ranging from 0.49 to 0.51 mg/L. For fosfomycin, the $Imax_{,F,PMB}$ values were 0.99, 0.81, and 0.89 for BRKP61, BRKP76, and KP0016-1, respectively, with IC50 values between 0.58 and 0.64 mg/L.

In contrast, incorporating mechanistic synergy did not improve the model fits for isolates BRKP67 and BRKP28, both of which harbored MgrB and porin mutations. Based on resistance gene profiles and model discrimination, KP0052-1, which lacked porin mutations, was well described by subpopulation synergy alone. Correlation coefficients between observed and model predicted log_{10} CFU/mL values were greater than 0.73 across all isolates, indicating good model performance: BRKP61 (0.79), BRKP76 (0.73),

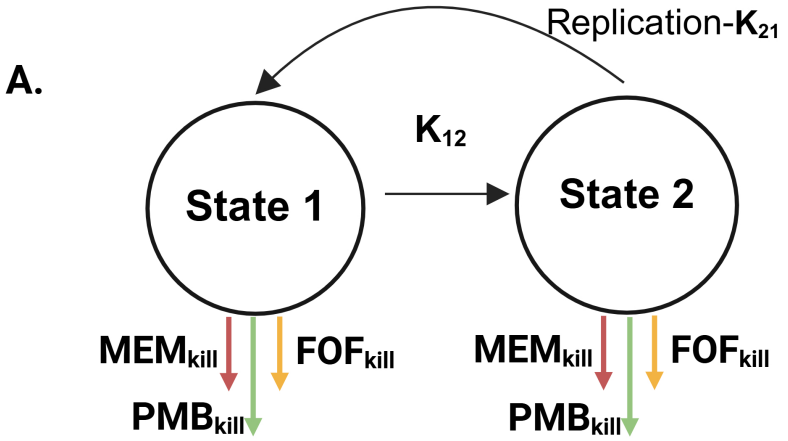

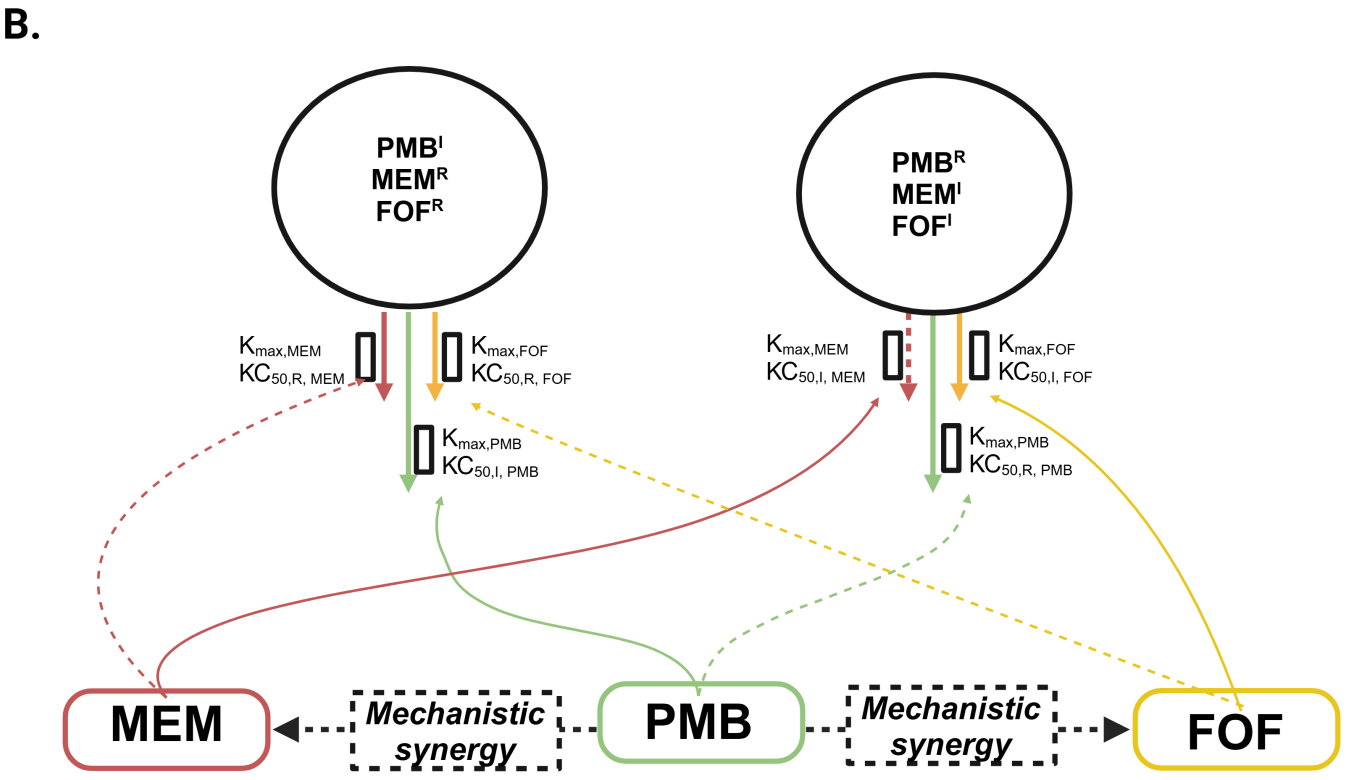

FIG 2 The mechanism-based PK/PD model structure describing the bacterial killing by meropenem (MEM_{kill}), polymyxin B (PMB_{kill}), and fosfomycin (FOF_{kill}) as monotherapy and in combination therapy. (A) A two-state bacterial life cycle model was utilized to describe the bacterial replication and drug effect of bacterial killing is on both state 1 and state 2 of life cycle model. (B) The first subpopulation $PMB^{I}/MEM^{R}/FOF^{R}$ is intermediately resistant to polymyxin B (PMB) and resistant to meropenem (MEM) and fosfomycin (FOF). The second subpopulation $PMB^{R}/MEM^{I}/FOF^{I}$ is resistant to polymyxin B (PMB) and intermediately resistant to meropenem (MEM) and fosfomycin (FOF). The maximum killing rate constants (K_{max}) and the associated concentrations causing 50% of K_{max} (KC_{50}) are explained in Table 2. The structure also depicts the shift in meropenem (MEM) and fosfomycin (FOF) KC_{50} resulting from the mechanistic synergy because of polymyxin B (PMB) impacting MEM/FOF – intermediate/resistant subpopulation.

KP0016-1 (0.84), KP0052-1 (0.74), BRKP67 (0.73), and BRKP28 (0.91) (Fig. S2). Parameter estimates for each isolate are provided in Table 2. Model predictions of bacterial load over time for triple combination (Fig. 3), double combination (Fig. S3), and monotherapy (Fig. S4) aligned well with the observed data.

TABLE 2 Final model parameter estimates

Parameter estimate (%CV)	BRKP61	BRKP76	KP0016-1	KP0052-1	BRKP67	BRKP28
Bacterial growth and subpopulations						
Bacterial initial inoculum (LogCFU0) [log_{10} CFU/mL]	6.11 (0.64)	6.18 (2.20)	6.0 (1.04)	5.86 (5.18)	5.93 (1.64)	6.32 (0.45)
Maximum population size (LogCFUmax) [log_{10} CFU/mL]	9.33 (1.87)	9.05 (1.24)	8.43 (2.51)	9.10 (1.32)	9.44 (2.02)	9.35 (0.39)
Replication rate constant (k21) [h^{-1}]	50 (fixed)	50 (fixed)	50 (fixed)	50 (fixed)	50 (fixed)	50 (fixed)
Mean generation time (MGT) [min]						
$PMB^I/MEM^R/FOF^R$	83.3 (3.73)	–[a]	–	–	–	–
$PMB^R/MEM^I/FOF^I$	13.5 (3.73)	–	–	–	–	–
$PMB^I/MEM^I/FOF^I$	–	72.1 (7.71)	98.3 (5.07)	43.3 (8.07)	32.3 (12.5)	–
$PMB^R/MEM^R/FOF^I$	–	–	–	–	–	44.25 (6.50)
$PMB^R/MEM^R/FOF^R$	–	30.92 (4.74)	69.26 (2.31)	32.5 (5.0)	31.9 (5.08)	19.1 (7.39)
Log mutant frequency at baseline (log_{10} MF)						
$PMB^R/MEM^I/FOF^I$	−5.10 (1.91)	–	–	–		–
$PMB^R/MEM^R/FOF^R$		−5.48 (2.40)	−4.29 (3.14)	−5.15 (2.64)	−4.80 (1.64)	−6.55 (15.4)
Drug effect of polymyxin B						
Maximum killing rate constant of polymyxin B ($Kmax_{PMB}$) [h^{-1}]	13.4 (2.76)	11.2 (15.7)	10.9 (9.31)	6.61 (5.84)	9.08 (6.68)	3.61 (13.4)
Polymyxin B concentration causing 50% of $Kmax_{PMB}$ in I ($KC_{50,PMB,I}$) [mg/L]	0.82 (3.53)	2.20 (17.8)	6.56 (13.7)	2.68 (14.2)	2.77 (6.59)	–
Polymyxin B concentration causing 50% of $Kmax_{PMB}$ in R ($KC_{50,PMB,R}$) [mg/L]	41.03 (5.83)	79.2 (5.75)	61.16 (7.32)	38.34 (7.18)	96.78 (7.07)	38.82 (13.35)
Hill coefficient of polymyxin B	0.64 (3.83)	1.01 (8.25)	1.09 (4.14)	0.79 (5.62)	0.82 (10.16)	1.44 (20.82)
Drug effect of meropenem						
Maximum killing rate constant of meropenem ($Kmax_{MEM}$) [h^{-1}]	2.13 (4.39)	5.41 (5.04)	1.56 (12.9)	3.05 (18.8)	4.16 (7.09)	3.70 (16.5)
Meropenem concentration causing 50% of $Kmax_{MEM}$ in I ($KC_{50,MEM,I}$) [mg/L]	24.7 (6.50)	18.9 (12.4)	112 (9.39)	44.2 (16.5)	8.91 (25.8)	–
Meropenem concentration causing 50% of $Kmax_{MEM}$ in R ($KC_{50,MEM,R}$) [mg/L]	61.4 (4.30)	328 (2.50)	424 (2.83)	284 (11.5)	227 (12.3)	228 (11.1)
Hill coefficient of meropenem	1.85 (6.54)	1.26 (6.10)	1.99 (9.72)	0.84 (11.6)	1.17 (8.20)	1.43 (12.2)
Drug effect of fosfomycin						
Maximum killing rate constant of fosfomycin ($Kmax_{FOF}$) [h^{-1}]	3.74 (7.62)	3.03 (6.57)	0.64 (8.00)	4.01 (16.4)	3.45 (11.7)	3.42 (7.37)
Fosfomycin concentration causing 50% of $Kmax_{FOF}$ in I ($KC_{50,FOF,I}$) [mg/L]	42.5 (7.57)	21.1 (10.2)	20.2 (7.54)	26.1 (30.4)	20.4 (22.2)	22.0 (20.6)
Fosfomycin concentration causing 50% of $Kmax_{FOF}$ in R ($KC_{50,FOF,R}$) [mg/L]	44.71 (4.26)	647.5 (2.82)	448 (7.89)	761.7 (22.9)	1000 (7.38)	1342 (15.9)
Hill coefficient of fosfomycin	0.61 (9.59)	0.64 (27.7)	0.79 (22.5)	0.77 (8.81)	0.36 (9.64)	0.35 (23.73)
Mechanistic synergy of polymyxin B on Meropenem						
Maximum fractional decrease of $KC_{50,MEM,I}$ and/or $KC_{50,MEM,R}$ by polymyxin B via outer membrane disruption ($Imax_{M,PMB}$)	0.84 (7.32)	0.83 (13.0)	0.88 (18.7)	–	–	–
Polymyxin B concentration causing 50% of $Imax_{M,PMB}$ ($IC50_{M,PMB}$) [mg/L]	0.51 (6.92)	0.49 (21.01)	0.50 (26.65)	–	–	–
Hill coefficient for the mechanistic synergy	0.88 (6.50)	0.54 (16.3)	0.63 (14.7)	–	–	–
Mechanistic synergy of polymyxin B on Fosfomycin						
Maximum fractional decrease of $KC_{50,FOF,I}$ and/or $KC_{50,FOF,R}$ by polymyxin B via outer membrane disruption ($Imax_{F,PMB}$)	0.99 (9.89)	0.81 (14.5)	0.89 (13.6)	–	–	–
Polymyxin B concentration causing 50% of $Imax_{F,PMB}$ ($IC50_{F,PMB}$) [mg/L]	0.64 (9.35)	0.58 (34.8)	0.59 (15.7)	–	–	–
Hill coefficient for the mechanistic synergy	0.72 (7.22)	0.52 (14.4)	0.56 (12.3)	–	–	–

(*Continued on next page*)

TABLE 2 Final model parameter estimates (*Continued*)

Parameter estimate (%CV)	BRKP61	BRKP76	KP0016-1	KP0052-1	BRKP67	BRKP28
Variability model						
Additive residual variability [log_{10} CFU/mL]	0.39 (7.07)	0.54 (6.63)	0.45 (5.67)	0.77 (6.37)	0.52 (6.85)	0.25 (5.02)

[a]–, parameter not part of the structural model for the corresponding strain.

Model predicted bacterial load reduction in critically ill patients

Simulations using a population PK model for critically ill patients showed median unbound polymyxin B exposures of 39.7 mg·h/L and 49.0 mg·h/L for recommended regimens: LD 2 mg/kg + MD 1.25 mg/kg q12h and LD 2.5 mg/kg + MD 1.5 mg/kg q12h, respectively. A previously recommended fixed dosing regimen (LD 150 mg + MD 75 mg q12h) yielded unbound polymyxin B exposure of 39.9 mg·h/L, similar to the lower bound of the range observed with the recommended weight-based regimen (17). A lower dose polymyxin B regimen (1 mg/kg q12h) resulted in a median exposure of 23.5 mg·h/L, which was 41%–52% lower than the recommended regimens. Fig. 4 presents box plots of percentage reduction in AUC_CFU for six isolates treated with double and triple combination therapy, and the time course log_{10} CFU/mL simulation data are shown in Fig. S5.

The double combination of polymyxin B (1 mg/kg q12h) with meropenem (2 g q8h) achieved <30% reduction in AUC_CFU for all six isolates; however, all isolates except BRKP28 exhibited an initial ~2 log_{10} CFU/mL reduction within the first 4 h, followed by regrowth Fig. S5. For BRKP61 isolate (bla_{KPC-2} + two porin mutations), the combination of polymyxin B (1 mg/kg q12h) with fosfomycin (8 g q8h) reduced AUC_CFU by 96.7%. The triple drug combination achieved a similar reduction (97.3%) when a lower fosfomycin dose (4 g q8h) was combined with lower meropenem (1 g q8h) and polymyxin B (1 mg/kg q12h) doses. Similarly, KP0052-1 (bla_{NDM-4} with no porin mutations) showed 85.3% reduction with polymyxin B (1 mg/kg q12h) and fosfomycin (8 g q8h), while the triple combination with same polymyxin B, fosfomycin doses and a lower meropenem dose (1 g q8h) resulted in a 93.1% reduction in AUC_CFU.

The double combination of polymyxin B (1 mg/kg q12h) and fosfomycin (8 g q8h) resulted in 74.3% and 73.0% reduction in AUC_CFU for BRKP76 (bla_{KPC-2} + three porin mutations) and BRKP67 (bla_{KPC-2} + two porin + *mgrB* mutations), respectively. Adding meropenem (1 g q8h) in the triple combination further improved the percentage reduction in AUC_CFU by ~1.1-fold (BRKP76: 87.0% and BRKP67: 81.8%).

For KP0016-1 (non-carbapenemase producer with three porin mutations), the triple drug combination with median unbound polymyxin B exposure of 23.5 mg·h/L resulted in only a 51.7% reduction in AUC_CFU. Increasing the median exposure to 49.0 mg·h/L enhanced the reduction to 67.7%. BRKP28, a strain resistant to all three tested antibiotics, exhibited only a modest reduction in bacterial load (20.9%) with fosfomycin alone or in combination with polymyxin B. The triple-drug regimen also failed to produce a meaningful reduction. Notably, fosfomycin alone led to a substantial initial decrease of 2–3 log_{10} CFU/mL within the first 8 h. Fig. 5 outlines the overall workflow for selecting polymyxin B-based combination therapy based on carbapenamase production and polymyxin B susceptibility.

DISCUSSION

The rising incidence of both carbapenemase producing and non-carbapenemase producing CRKP infections, coupled with a lack of effective treatment options, underscores the need for detailed *in vitro* evaluation of potential treatment regimens using currently approved drugs. Although newer β-lactams/β-lactamase inhibitor combinations are recommended for treating carbapenemase producing CRKP, there is increasing evidence of resistance due to overexpressed efflux pumps, porin loss, or mutations in carbapenemases (18–21). Several studies have investigated the efficacy of polymyxin B-based combinations against NDM-producing *K. pneumoniae,* reinforcing polymyxin's

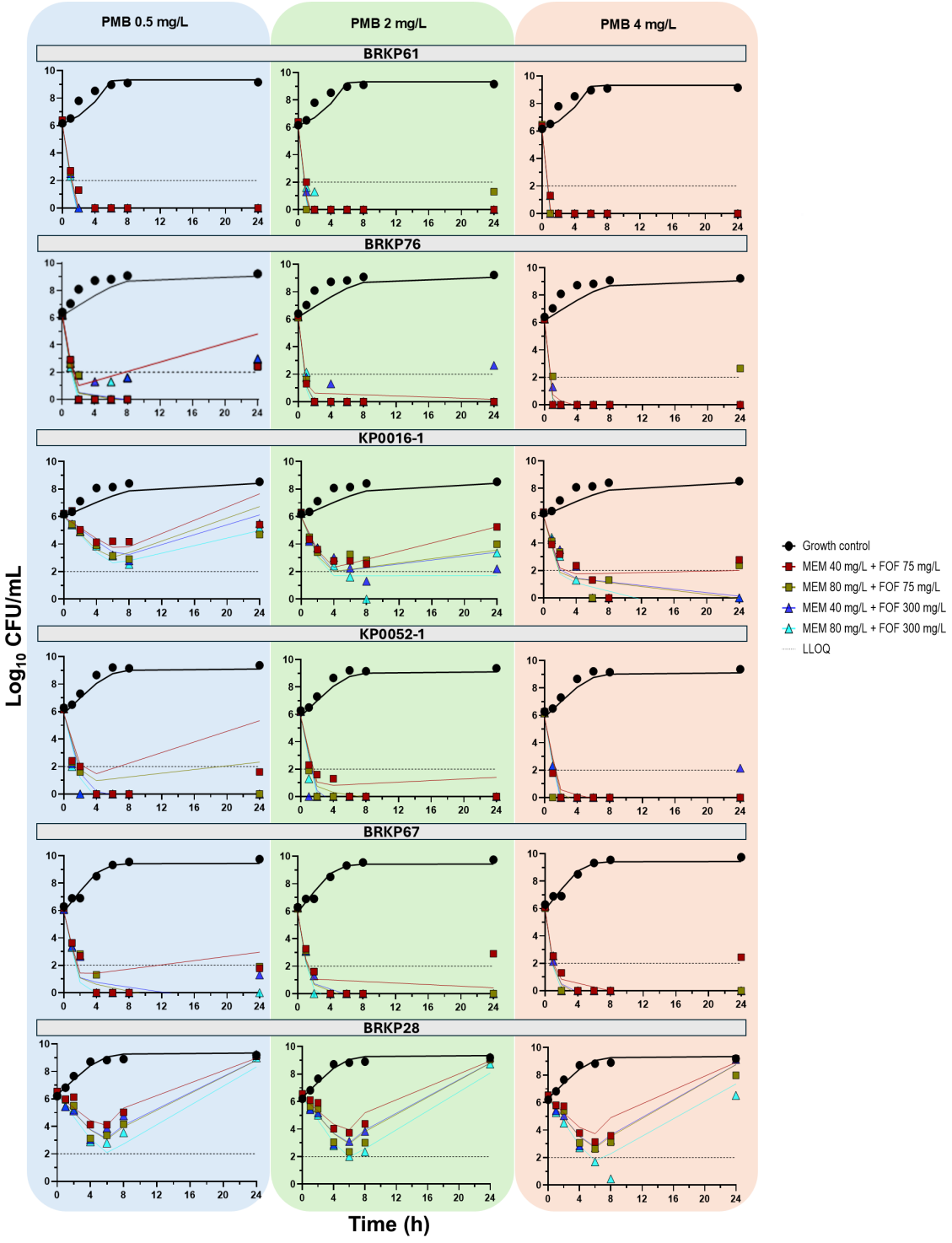

FIG 3 The model predictions for triple combination therapy with polymyxin B 0.5 mg/L, 2 mg/L, and 4 mg/L for six isolates are shown. The solid line represents the model predictions, while the symbols indicate the observed data. The horizontal dotted line marks the LLOQ (2 $\log_{10}$ CFU/mL).

role as a last-line agent for these difficult-to-treat pathogens (22–24). Observational clinical data also supports the use of meropenem containing combinations, which have been associated with lower mortality rates (25). Additionally, a small prospective study found that intravenous fosfomycin-based combination therapy reduced all-cause hospital mortality in critically ill patients with CRKP infections (26).

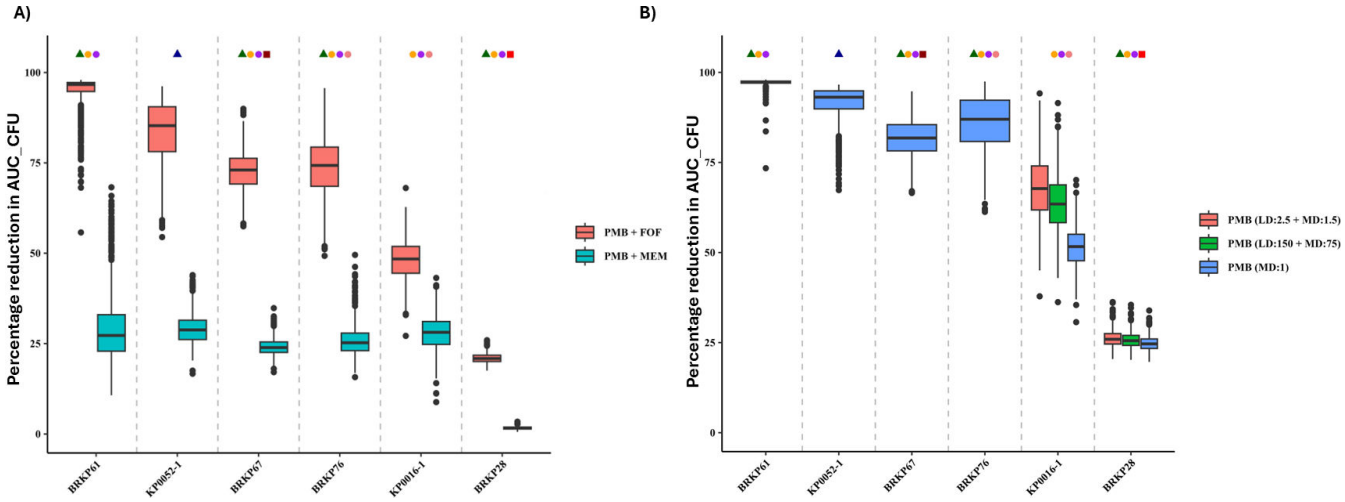

FIG 4 Box plots showing the percentage reduction in AUC_CFU for (A) double combination therapy with polymyxin B (1 mg/kg q12h) + meropenem (2 g q8h) or fosfomycin (8 g q8h) (B) Box plots showing the percentage reduction in AUC_CFU for triple combination therapy with different polymyxin B regimens. Fosfomycin was administered at 4 g q8h for BRKP61 and 8 g q8h for all other isolates. Meropenem was administered at 2 g q8h for two isolates KP0016-1 and BRKP28 and 1 g q8h for all other isolates. Green and blue triangle represents isolates with bla_{KPC-2} and bla_{NDM-4} respectively. Orange, purple, and brown circles indicate the presence of *ompK-35, ompK-36,* and *ompK-37* mutations, respectively. The brown square represents the insertion of ISKpn13 (1,148 bp), an IS5-like element in the *mgrB*, with a polymyxin B MIC of 8 mg/L. The red square represents a premature stop codon in the MgrB protein, with a polymyxin B MIC of > 128 mg/L.

Meropenem and fosfomycin were selected for their different but complementary mechanisms of action: meropenem inhibits peptidoglycan synthesis by binding to penicillin-binding proteins, while fosfomycin prevents the transpeptidation of peptidoglycan, an earlier step in peptidoglycan biosynthesis. Both drugs are hydrophilic, and mutations in outer membrane porins can hinder their ability to penetrate and achieve adequate exposure at the site of infection. Polymyxin B, through its detergent-like disruption of the outer membrane, enhances the intracellular accumulation of meropenem and fosfomycin (22, 27). Recent Infectious Diseases Society of America (IDSA) guidance does not recommend polymyxin-based combination regimens for CRE infections due to the increased toxicity associated with this narrow therapeutic index drug (2). Despite these concerns over nephrotoxicity, various clinical trials like OVERCOME and AIDA have demonstrated reduced mortality in CRE with polymyxin-based combination therapies (14, 15).

To assess the synergistic potential of polymyxin B with meropenem and/or fosfomycin, we selected six different isolates with varying phenotypic and genotypic resistance mechanisms. These included strains harboring carbapenemases like bla_{KPC-2} or bla_{NDM-4}, with or without porin mutations that confer resistance to meropenem. Fosfomycin uptake is facilitated by *ompF* in *E. coli,* a homolog of *ompK35* in *K. pneumoniae* (28)*;* five of the six isolates had *ompK35* mutations, potentially limiting fosfomycin penetration. Two isolates also carried *MgrB* mutations, one of which (BRKP28) exhibited extreme phenotypic resistance to polymyxin B (>128 mg/L) (Table S2).

Information about phenotypic and genotypic resistance mechanisms provided significant insights into the mechanistic synergy in MBM across the six isolates. Based on the presence of porin mutations and polymyxin B susceptibility, mechanistic synergy was applicable to only three isolates. Our model estimated 83%–88% mechanistic synergy for polymyxin B with meropenem and 81%–98% with fosfomycin. While polymyxin B-meropenem combinations demonstrated >80% synergy, they did not produce meaningful reduction in AUC_CFU. Importantly, the synergistic effect was evident as an initial ~2 $\log_{10}$ CFU/mL reduction within the first 4 h for most isolates. This early bactericidal activity could be clinically relevant, particularly when considered in the context of host immune response. However, in the time-kill approach, this initial strong

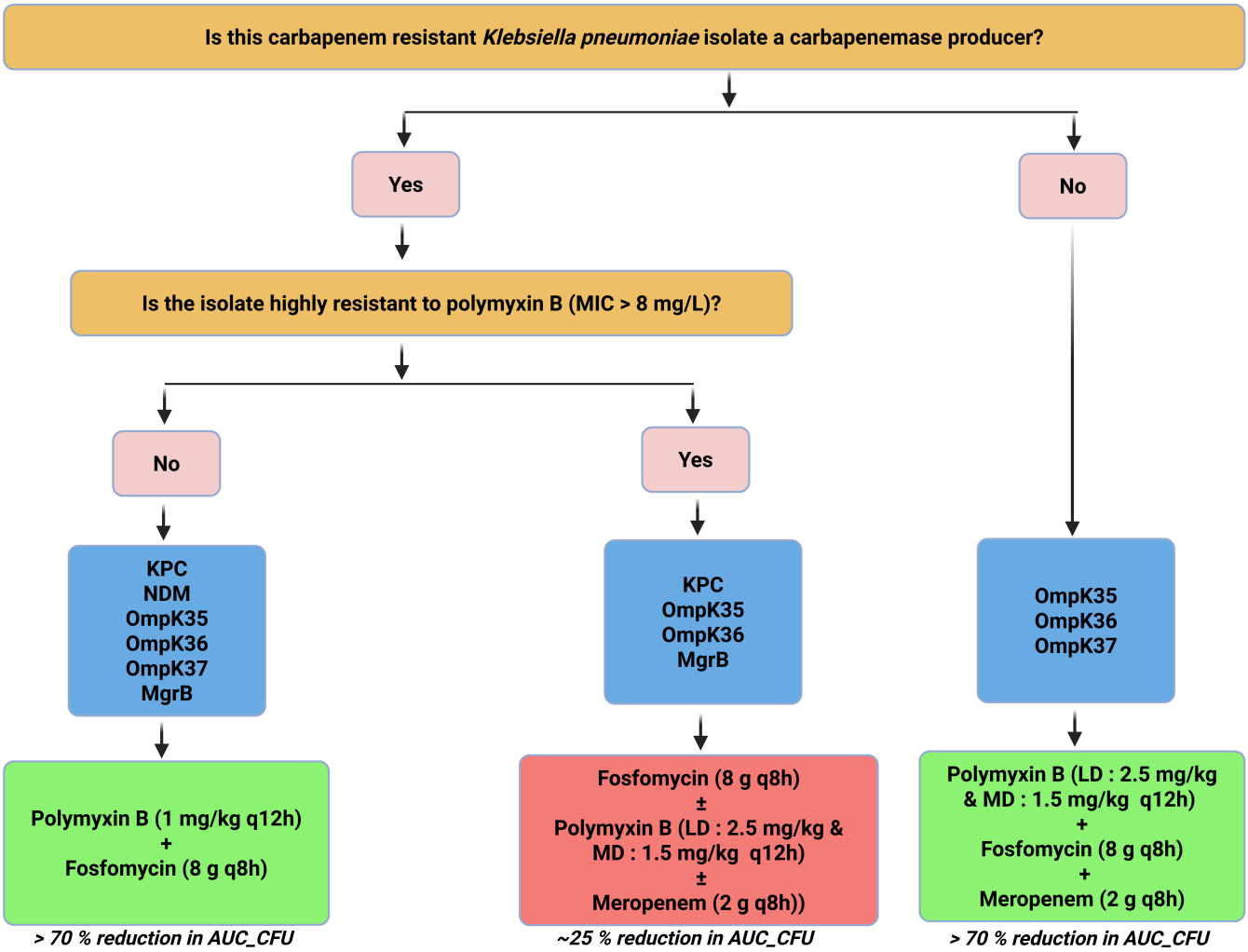

FIG 5 Workflow for selecting polymyxin B-based combination therapy. The decision pathway is based on carbapenemases production and polymyxin B susceptibility. Yellow boxes represent the critical questions used to determine the treatment regimens. Pink boxes represent decision points. Blue boxes show the different resistance genes present among the six isolates. Green boxes represent treatment regimens that were successful, achieving > 70% reduction in AUC_CFU. Red box indicates an unsuccessful treatment regimen, with only a 25% reduction in AUC_CFU.

activity is followed by complete regrowth. Therefore, further *in vivo* studies evaluating this combination may give some insights into treatment optimization with this combination. In contrast, the 81%–98% synergy of polymyxin B-fosfomycin combinations led to substantial AUC_CFU reductions for four isolates.

Findings from the present study collectively guided the development of a decision-support workflow (Fig. 5), to inform antibiotic selection based on carbapenemase production and polymyxin B susceptibility for clinical use or further dynamic *in vitro* evaluation (e.g., hollow fiber infection models). Alternative dosing strategies, such as front-loading polymyxin B or site-specific administration (e.g., inhaled polymyxin B for lung infections), may further enhance therapeutic efficacy (23).

The early bactericidal activity observed with the polymyxin B–meropenem combination in the present study may have clinical relevance; however, the subsequent regrowth underscores the challenge of managing CRKP infections with this regimen in the USA, where IV fosfomycin is not yet approved. Notably, a clinical trial of IV fosfomycin (ZTI-01) for complicated urinary tract infections and pyelonephritis demonstrated favorable efficacy and safety (29). Fosfomycin monotherapy against BRKP28 isolate showed substantial initial decrease of 2-3 $\log_{10}$ CFU/mL within the first 8 h, which

could be clinically meaningful when considering the host immune response. However, in the time-kill assay, where immune factors are absent, this early bactericidal effect was followed by complete bacterial regrowth. The addition of polymyxin B did not alter the regrowth pattern, suggesting that the current antibiotic combinations lack sustained efficacy against this strain. Hence, further investigation into β-lactam/β-lactamase inhibitor combinations administered 8 h after initial fosfomycin-based treatment in *in vivo* models may offer promising therapeutic insights for treating BRKP28 effectively.

In the present study, polymyxin B-based combinations were effective against all isolates except BRKP28. This is likely due to uncharacterized resistance mechanisms, possibly involving positively charged lipopolysaccharide (LPS) that interferes with polymyxin B's interaction with LPS. Resistance to polymyxin B is increasingly reported and is often driven by mutations in two-component systems (TCS) such as *PhoP/PhoQ* and *PmrA/PmrB*, which regulate the expression of genes involved in LPS modification. These mutations result in the addition of cationic groups such as 4-amino-4-deoxy-L-arabinose (L-Ara4N) or phosphoethanolamine (PEtn) to lipid A, reducing the net negative charge of the bacterial surface and weakening electrostatic interactions with polymyxins (30). Additionally, loss of *mgrB*, a negative regulator of the *PhoQ/PhoP* pathway, further enhances L-Ara4N modification of lipid A. Such alterations of polymyxin B's target in LPS contribute to increased resistance to polymyxins (31).

Despite these resistance mechanisms, combination therapies remain effective. For example, a recent study found that the triple combination therapy with polymyxin B, meropenem and fosfomycin significantly suppressed the selective amplification of polymyxin B resistant subpopulations in *Acinetobacter baumannii* infections (32). Consistent with this, our results demonstrate that polymyxin B-based combinations are effective against polymyxin-resistant isolate like BRKP67, suggesting that the polymyxin B MIC (i.e., phenotypic susceptibility) alone may not be predictive of the pharmacodynamic response. Supporting this, MacNair et al. reported that *Enterobacteriaceae* strains harboring *mcr-1* did not impede colistin's ability to disrupt the outer membrane, indicating that acquired resistance to polymyxins does not necessarily hinder its synergistic potential in combination (33). Similarly, Sharma et al. observed extensive morphological changes in all isolates except BRKP28 following polymyxin B exposure (27).

Concerns about nephrotoxicity with higher polymyxin B exposure remain. Tailored polymyxin B-based combination therapy is essential to ensure efficacy while minimizing the risk for nephrotoxicity (23). A retrospective study in adult patients found a 50% probability of polymyxin B-associated acute kidney injury when trough concentrations (total drug) ≥3.13 mg/L (34). Our simulations showed that a low-dose polymyxin B regimen (1 mg/kg every 12 h) maintained trough concentrations below the nephrotoxic threshold while still achieving synergistic effects. Given fosfomycin's favorable safety profile, its maximum recommended dose (8 g every 8 h) should be used to maximize synergistic effects. In cases requiring triple combination therapy, adding low dose meropenem (1 g every 8 h) or the recommended meropenem regimen (2 g every 8 h) is necessary to achieve bacterial reduction. Both meropenem regimens maintained trough concentrations (total drug) below the nephrotoxic (44.5 mg/L) and neurotoxic (64.5 mg/L) thresholds (35) (Fig. S1).

Dosing strategies recommended in this study were derived from our MBM, which applied a consistent structural growth model across all six isolates, incorporating distinct subpopulation dynamics and drug-specific killing effects. While our findings align with prior systematic reviews addressing therapeutic approaches for multidrug-resistant Gram-negative bacteria (36, 37) and our modeling approach mirrors previous MBM applications, its generalizability is limited by the resistance mechanisms expressed by each strain and its polymyxin B susceptibility. In contrast, a prior MBM model developed using six *E. coli* isogenic strains, successfully generalized to predict ciprofloxacin efficacy in additional strains not used in model development. The study employed a similar structural framework across strains and allowed potency parameters (EC50) to vary,

reflecting differences in susceptibility, and accurately predicted outcomes under varied inoculum conditions (38). Similarly, another study integrated clinical PK/PD data from the AIDA trial into MBM, incorporating isolate-specific drug effect parameters, and found a correlation between individualized predictions of bacterial burden and clinical trial outcomes (39).

Future studies should expand evaluation of polymyxin B-based combinations and novel β-lactamase inhibitors across a broader panel of CRKP isolates with diverse genotypes. Furthermore, the mechanism-based model can be improved by integrating multi-omics data to enhance understanding of how specific resistance mechanisms influence drug pharmacodynamic activity in monotherapy and combination regimens to improve the applicability of a MBM approach to select therapies effective against more strains with different resistance mechanism.

MATERIALS AND METHODS

Antimicrobials and media

Mueller-Hinton broth (MHB; Becton Dickinson, Franklin Lakes, NJ) supplemented with calcium and magnesium (CAMHB; 25.0 mg/L Ca^{2+}, 12.5 mg/L Mg^{2+}) and Mueller-Hinton II agar (MHA; Becton, Dickinson, Franklin Lakes, NJ) were used for susceptibility testing and all *in vitro* experiments. CAMHB was further supplemented with 25 mg/L glucose-6-phosphate (G-6-P) (lot number 343234, Acros Organics). The inclusion of G-6-P enhances the *in vitro* activity of fosfomycin, aligning it more closely with *in vivo* efficacy. This is because G-6-P compensates for reduced bacterial uptake of fosfomycin caused by the presence of glucose and phosphate in Mueller-Hinton agar (40). Stock solutions of polymyxin B (lot number WXBB5309V; Sigma Aldrich, St. Louis, MO), meropenem (lot number LC24337; AK Scientific, Union City, CA) and fosfomycin (lot number: K001, Nabriva Therapeutics US, Inc., Fort Washington, PA) were freshly prepared in sterile water and saline prior to each experiment. All drug solutions were filter sterilized with a 0.22 µm filter (Fisher Scientific, Pittsburgh, PA).

Bacterial isolates and antibiotic susceptibility testing

Four clinical CRKP isolates used in this study (BRKP28, BRKP61, BRKP67, BRKP76) were obtained from individual patients at Instituto Dante Pazzanese de Cardiologia (Sao Paulo, Brazil), while two additional isolates (KP0016-1 and KP0052-1) were obtained from Siriraj Hospital (Bangkok, Thailand) (27). Polymyxin B and meropenem MICs were determined in triplicate using the broth microdilution method, whereas fosfomycin susceptibility was assessed using the agar dilution method, both following CLSI guidelines (41). MIC interpretations for polymyxin B and meropenem were based on CLSI breakpoints for *K. pneumoniae*. Since CLSI does not provide breakpoints for fosfomycin against *K. pneumoniae*, EUCAST for intravenous fosfomycin against *E. coli* were used as a reference (42).

Genomic characterization

Polymerase chain reaction (PCR) was performed using previously described primer sets for β-lactamase Ambler classes A (bla_{GES} and bla_{KPC}), B (bla_{NDM-1}, bla_{VIM}, and bla_{IMP}), and D (bla_{OXA-48} and bla_{OXA-40}) (43). Primers used in amplification experiments to identify *mgrB* (31) and *ompK* genes (44) (*ompK35*, *ompK36,* and *ompK37*) are listed in Table S1. Isolates were also characterized for the virulence genes and the primers used for the virulence genes are mentioned in Table S1. Genomic DNA was extracted from bacterial isolates using the Purelink Genomic DNA Mini kit (Invitrogen, Carlsbad, CA). PCRs were performed using Q5 Hi-Fidelity Taq DNA Polymerase (New England Biolabs, Ipswich, MA). Reactions were carried out in an Eppendorf Mastercycler (Eppendorf, Hamburg, Germany), and PCR products were analyzed by direct sequencing (GENEWIZ,

Research Triangle Park, NC). Nucleotide and deduced protein sequences were analyzed using BLAST (http://blast.ncbi.nlm.nih.gov/).

Static concentration time-kill assays

SCTK assays were conducted over a 24 h period to evaluate the rate and extent of killing by monotherapy, double and triple combinations using polymyxin B, meropenem, and fosfomycin. PK/PD analysis was performed using six isolates at a starting inoculum of ~10^6 CFU/mL (CFU_0), as previously described (45). Antibiotic concentrations selected included both clinically achievable (polymyxin B: 0.5, 1, 2, 4, 8 mg/L; meropenem: 10, 20, 40 mg/L; Fosfomycin: 75, 150, 300, 500 mg/L) and supra-therapeutic (polymyxin B: 16 and 64 mg/L; meropenem: 60 and 120 mg/L) free-drug concentrations (i.e., unbound plasma concentrations) to characterize the concentration-response relationship against each isolate. Clinically relevant concentrations were selected based on maximum plasma concentrations (Cmax) reported in previously published population PK studies (17, 46, 47). Serial samples were obtained at 0, 1, 2, 4, 6, 8, and 24 h for bacterial quantification, with a lower limit of quantification (LLOQ) of 2 $\log_{10}$ CFU/mL.

Pharmacodynamic analysis

The pharmacodynamic effect was quantified as the change in $\log_{10}$ CFU/mL at 24 h (CFU_{24}) compared to baseline (CFU_0) (i.e., 24 h $\log_{10}$ CFU/mL reduction). Bactericidal activity was defined as a ≥ 3 $\log_{10}$ reduction at 24 h compared to the initial inoculum. To further assess bacterial killing in the polymyxin B-based combination therapy, AUC_CFU from 0 to 24 hours was calculated for both the double and triple drug combinations at static concentrations.

Mechanism based PK/PD model development

Mechanism-based PK/PD model was developed using the SCTK time course data describing the change in bacterial burden over time in response to antibiotic treatment against the six bacterial isolates. A life cycle model was used to describe the bacterial growth and replication for each bacterial isolate (48). The model included the transition of bacterial cells from vegetative state, preparing for replication (state 1), to the replication state, immediately prior to replication step (state 2).

A mixture model with pre-existing subpopulations with differing susceptibilities to polymyxin B, meropenem, and fosfomycin was considered to account for heterogeneity in the bacterial inoculum. Models with two, three, and four bacterial subpopulations were explored (49). The final model included two subpopulations with differing susceptibilities to polymyxin, meropenem, and fosfomycin for each isolate (equation 1).

$$CFU_{tot} = CFU_{IRR,1} + CFU_{IRR,2} + CFU_{RII,1} + CFU_{RII,2} \quad (1)$$

where CFU_{tot} is the total viable bacterial concentration, CFU_{IRR} is the polymyxin B-intermediate, meropenem-resistant and fosfomycin-resistant subpopulation. CFU_{RII} is the polymyxin B-resistant, meropenem-intermediate and fosfomycin-intermediate subpopulation. Each of the bacterial subpopulations, $CFU_{IRR,1}$ and $CFU_{IRR,2}$, is in vegetative (state 1) and replicative state (state 2) respectively. The differential equation for the two states describing the bacteria in state 1 and 2 for subpopulation CFU_{IRR} with killing by polymyxin B (PMB), meropenem (MEM), and fosfomycin (FOF) is shown in equations 2 and 3.

$$\frac{d(CFU_{IRR,1})}{dt} = REP \cdot k_{21} \cdot CFU_{IRR,2} - k_{12,IRR} \cdot CFU_{IRR,1} - (Kill_{PMB,I} + Kill_{MEM,R} + Kill_{FOF,R}) \cdot CFU_{IRR,1}, \left(IC_{CFU_{IRR,1}} = CFU_0 \cdot MF_{IRR}\right) \quad (2)$$

$$\frac{d(CFU_{IRR,2})}{dt} = -k_{21}\cdot CFU_{IRR,2} + k_{12,IRR}\cdot CFU_{IRR,1} - (Kill_{PMB,I} + \mathrm{Kill}_{MEM,R} + \mathrm{Kill}_{FOF,R})\cdot CFU_{IRR,2}, \left(IC_{CFU_{IRR,2}} = 0\right) \quad (3)$$

where REP is the replication factor defined as $2\cdot\left(1-\frac{CFU_{tot}}{CFU_{MAX}+CFU_{tot}}\right)$, CFU_{MAX} is the maximum bacterial population size and 2 represents the doubling of bacteria during replication. The inverse of the mean replication time from state 2 to state 1, k_{21} was fixed to 50 h^{-1} (49, 50). $k_{12,\ IRR}$, the inverse of mean replication time from state 1 to state 2 was estimated for each subpopulation. $Kill_{PMB,I}$, $Kill_{MEM,R}$, and $Kill_{FOF,R}$ are the killing rate by polymyxin B, meropenem, and fosfomycin, respectively for CFU_{IRR} subpopulation. The killing activity of each drug is described by the Hill equation as shown in equation 4.

$$Kill_{\mathrm{drug}} = \frac{K_{MAX,\mathrm{drug}}\cdot \mathrm{drug}^{\mathrm{h}}}{\left(KC_{50,\mathrm{drug}}\right)^{h} + \mathrm{drug}^{\mathrm{h}}} \quad (4)$$

where drug can be concentration of polymyxin B, meropenem, or fosfomycin; $K_{MAX,drug}$ is the maximum killing rate constant of drug; $KC_{50,drug}$ is the drug concentration causing 50% of $K_{MAX,drug}$; h is the Hill coefficient. We considered subpopulation synergy (i.e., polymyxin B killing bacteria resistant to meropenem/fosfomycin and vice versa) in this model. We estimated the total initial inoculum ($\log_{10}CFU_0$) and the log transformed mutation frequency (MF) for the subpopulations. Initial conditions were implemented as described previously (49).

The interaction between polymyxin B and meropenem and/or fosfomycin was modeled using a Hill function to describe the mechanistic synergy based on polymyxin B's effect on the outer membrane of the Gram-negative bacteria. This synergy increases the target site concentration of meropenem and fosfomycin, thereby enhancing the sensitivity of the intermediate and resistant subpopulations to meropenem and fosfomycin ($KC_{50,MEM,I}$, $KC_{50,FOF,I}$, $KC_{50,MEM,R}$, $KC_{50,FOF,R}$). Equation 5 describes the mechanistic synergy by polymyxin B, and equations 6 and 7 describes the impact of mechanistic synergy on meropenem intermediate and fosfomycin resistant subpopulation, respectively.

$$\mathrm{Mechanistic\_synergy} = 1 - \left(\frac{I_{MAX}\cdot (C_{PMB})^{h}}{(C_{PMB})^{h} + (IC_{50})^{h}}\right) \quad (5)$$

$$Kill_{MEM,I} = \frac{K_{MAX,MEM}\cdot MEM^{h}}{\left(KC_{50,MEM,I}\cdot Mechanistic\_synergy\right)^{h} + MEM^{h}} \quad (6)$$

$$Kill_{FOF,R} = \frac{K_{MAX,FOF}\cdot FOF^{h}}{\left(KC_{50,FOF,R}\cdot \mathrm{Mechanistic\_synergy}\right)^{h} + FOF^{h}} \quad (7)$$

Where I_{MAX} is the maximum fractional decrease in $KC_{50,MEM,I}$ and $KC_{50,FOF,R}$ by polymyxin B causing disruption of the bacterial outer membrane, IC_{50} is the polymyxin B concentration causing 50% of I_{MAX}, h is the hill coefficient.

The residual unexplained variability for $\log_{10}$ transformed bacterial load data was explained by additive error model. Observations below the LLOQ were fit using the Beal M3 (51). Parameter estimation was performed using the importance sampling algorithm (pmethod = 4) in S-ADAPT (version 1.57) facilitated by SADAPT-TRAN (52). Models were evaluated based on model fits, diagnostic plots, precision of parameter estimates, and objective function value (OFV).

Monte Carlo simulations to predict drug response in clinical practice

Monte Carlo simulations were performed for 1,000 adult patients using mrgsolve R package. Previously published population PK models for polymyxin B (17), meropenem (46), and fosfomycin (47) in critically ill patients were used to simulate the unbound

plasma concentrations taking inter individual variability into consideration (Fig. S1). The unbound plasma concentrations were determined using published fraction unbound (*fu*) for polymyxin B = 0.42 and meropenem = 0.98, while plasma protein binding for fosfomycin was negligible. These simulated unbound drug concentrations were linked to the developed MBM to predict impact on bacterial killing in critically ill patients. Simulations were performed using demographics within the reported range in the population PK models for polymyxin B, meropenem, and fosfomycin [bodyweight of 70 kg, serum albumin of 2.8 g/dl, and creatinine clearance of 90 mL/min].

The efficacy of a lower polymyxin B dosing regimen (1 mg/kg every 12 h as 1 h infusion) was evaluated in both the double and triple combination regimens. In cases where the lower dosing regimen did not result in a significant reduction in AUC_CFU, simulations were performed using the recommended weight-based polymyxin B regimen (2.5 mg/kg loading dose [LD] followed by 1.5 mg/kg every 12 h maintenance dose [MD] as 1 h infusion) and a fixed regimen (150 mg LD and 75 mg every 12 h MD as 1 h infusion). Additionally, meropenem (1 g or 2 g every 8 h as 3 h infusion) and fosfomycin (4 g or 8 g every 8 h as 3 h infusion) regimens were simulated. The pharmacodynamic activity of double and triple combination therapy was evaluated as a percentage reduction in AUC_CFU with the treatment of interest compared to no treatment.

Conclusion

While the importance of appropriate antimicrobial therapy is well recognized, high-quality evidence to guide antibiotic selection for extensively drug resistant CRE isolates is limited. Addressing this gap, a key contribution of this work is the development of a mechanism-based PK/PD model informed by resistance mechanisms. Model-based simulations, leveraging clinical drug exposure from published population PK model, enabled prediction of pharmacodynamic responses in critically ill patients. Notably, our findings indicate that a low-dose polymyxin B regimen (1 mg/kg q12h) can produce synergistic effects when combined with appropriate companion antibiotic(s) while minimizing nephrotoxicity. Such combinations can be effective in managing infections caused by both carbapenamase producing and non-producing CRKP, strains including those resistant to polymyxin B.

Our results also suggest that polymyxin B shows greater synergy with fosfomycin than with meropenem. Triple combination therapy involving polymyxin B, meropenem, and fosfomycin may be particularly beneficial for non-carbapenamase producing isolates resistant to newer antibiotics. Understanding the underlying resistance mechanisms is essential for designing treatment regimens that combine both older and newer antibiotics to achieve adequate exposure at the infection site.

Future research should focus on integrating genotype-phenotype associations with quantitative pharmacodynamic data, especially to evaluate drug activity in the presence or absence of specific resistance genes. Given the limited clinical data, a systematic and rational approach to generating robust nonclinical PK/PD evidence is critical for preserving the effectiveness of our current antibiotic arsenal.

AUTHOR AFFILIATIONS

[1]Titus Family Department of Clinical Practice, USC Alfred E. Mann School of Pharmacy and Pharmaceutical Sciences, University of Southern California, Los Angeles, California, USA
[2]Division of Pharmaceutics and Experimental Therapeutics, Eshelman School of Pharmacy, University of North Carolina at Chapel Hill, Chapel Hill, North Carolina, USA
[3]Department of Pharmacy, Fujian Medical University Union Hospital, Fuzhou, People's Republic of China
[4]College of Pharmacy, Fujian Medical University, Fuzhou, People's Republic of China
[5]Instituto Dante Pazzanese de Cardiologia, São Paulo, Brazil

[6]Antimicrobianos, Instituto Nacional de Enfermedades Infecciosas, Antimicrobial Service of the National Institute of Infectious Diseases (ANLIS Dr. Carlos G. Malbrán), Buenos Aires, Argentina
[7]Center for Applied Biotechnology Studies, Department of Biological Science, College of Natural Sciences and Mathematics, California State University Fullerton, Fullerton, California, USA
[8]Division of Allergy, Immunology and Infectious Diseases, Rutgers Robert Wood Johnson Medical School, New Brunswick, New Jersey, USA
[9]Department of Molecular Biology and Microbiology, Case Western Reserve University School of Medicine, Cleveland, Ohio, USA
[10]CWRU-Cleveland VAMC Center for Antimicrobial Resistance and Epidemiology (Case VA CARES), Cleveland, Ohio, USA
[11]Geriatric Research Education and Clinical Center, Louis Stokes Cleveland Department of Veterans Affairs Medical Center, Education and Clinical Center, Cleveland, Ohio, USA
[12]Department of Medicine, Case Western Reserve University School of Medicine, Cleveland, Ohio, USA
[13]Departments of Pharmacology, Biochemistry, Proteomics and Bioinformatics, Case Western Reserve University School of Medicine, Cleveland, Ohio, USA

AUTHOR ORCIDs

Ramya Mahadevan http://orcid.org/0009-0008-3951-1146
Hongqiang Qiu http://orcid.org/0000-0003-3285-8768
Maria Soledad Ramirez http://orcid.org/0000-0002-9904-7890
Robert A. Bonomo http://orcid.org/0000-0002-3299-894X
Gauri G. Rao http://orcid.org/0000-0002-8704-7770

AUTHOR CONTRIBUTIONS

Ramya Mahadevan, Data curation, Formal analysis, Methodology, Visualization, Writing – original draft, Writing – review and editing | Estefany Garcia, Data curation, Formal analysis, Visualization, Writing – original draft | Rajnikant Sharma, Data curation, Writing – review and editing | Hongqiang Qiu, Data curation | Ahmed Elsheikh, Data curation | Robert Parambi, Data curation, Formal analysis | Cely Saad Abboud, Writing – review and editing | Fernando Pasteran, Writing – review and editing | Maria Soledad Ramirez, Writing – review and editing | Keith S. Kaye, Writing – review and editing | Robert A. Bonomo, Writing – review and editing | Gauri G. Rao, Conceptualization, Data curation, Methodology, Resources, Supervision, Visualization, Writing – review and editing

ADDITIONAL FILES

The following material is available online.

Supplemental Material

Supplemental figures and tables (AAC00782-25-s0001.docx). Figures S1-S5 and Tables S1 and S2.

REFERENCES

1. Wise MG, Karlowsky JA, Mohamed N, Hermsen ED, Kamat S, Townsend A, Brink A, Soriano A, Paterson DL, Moore LSP, Sahm DF. 2024. Global trends in carbapenem- and difficult-to-treat-resistance among World Health Organization priority bacterial pathogens: ATLAS surveillance program 2018–2022. J Glob Antimicrob Resist 37:168–175. https://doi.org/10.1016/j.jgar.2024.03.020
2. Tamma PD, Heil EL, Justo JA, Mathers AJ, Satlin MJ, Bonomo RA. 2024. Infectious diseases society of America 2024 guidance on the treatment of antimicrobial-resistant gram-negative infections. Clin Infect Dis:ciae403. https://doi.org/10.1093/cid/ciae403
3. Timbrook TT, Morton JB, McConeghy KW, Caffrey AR, Mylonakis E, LaPlante KL. 2017. The effect of molecular rapid diagnostic testing on clinical outcomes in bloodstream infections: a systematic review and meta-analysis. Clin Infect Dis 64:15–23. https://doi.org/10.1093/cid/ciw649
4. Evans SR, Hujer AM, Jiang H, Hujer KM, Hall T, Marzan C, Jacobs MR, Sampath R, Ecker DJ, Manca C, Chavda K, Zhang P, Fernandez H, Chen L, Mediavilla JR, Hill CB, Perez F, Caliendo AM, Fowler VG Jr, Chambers HF, Kreiswirth BN, Bonomo RA, Antibacterial Resistance Leadership Group. 2016. Rapid molecular diagnostics, antibiotic treatment decisions, and

developing approaches to inform empiric therapy: PRIMERS I and II. Clin Infect Dis 62:181–189. https://doi.org/10.1093/cid/civ837
5. Bonnin RA, Jeannot K, Santerre Henriksen A, Quevedo J, Dortet L. 2025. *In vitro* activity of cefepime-enmetazobactam on carbapenem-resistant Gram negatives. Clin Microbiol Infect 31:240–249. https://doi.org/10.1016/j.cmi.2024.09.031
6. Bhowmick T, Canton R, Pea F, Quevedo J, Santerre Henriksen A, Timsit J-F, Kaye KS. 2025. Cefepime-enmetazobactam: first approved cefepime-β- lactamase inhibitor combination for multi-drug resistant *Enterobacterales*. Future Microbiol 20:277–286. https://doi.org/10.1080/17460913.2025.2468112
7. Koenig C, Kuti JL. 2024. Evolving resistance landscape in gram-negative pathogens: an update on β-lactam and β-lactam-inhibitor treatment combinations for carbapenem-resistant organisms. Pharmacotherapy 44:658–674. https://doi.org/10.1002/phar.2950
8. Lin CK, Page A, Lohsen S, Haider AA, Waggoner J, Smith G, Babiker A, Jacob JT, Howard-Anderson J, Satola SW. 2024. Rates of resistance and heteroresistance to newer β-lactam/β-lactamase inhibitors for carbapenem-resistant Enterobacterales. JAC Antimicrob Resist 6:dlae048. https://doi.org/10.1093/jacamr/dlae048
9. NIAID. 2019. NIAID's antibiotic resistance research framework: current status and future directions. Bethesda, MD, USA National Institute of Allergy and Infectious Diseases
10. Falagas ME, Lourida P, Poulikakos P, Rafailidis PI, Tansarli GS. 2014. Antibiotic treatment of infections due to carbapenem-resistant *Enterobacteriaceae*: systematic evaluation of the available evidence. Antimicrob Agents Chemother 58:654–663. https://doi.org/10.1128/AAC.01222-13
11. Sheu C-C, Chang Y-T, Lin S-Y, Chen Y-H, Hsueh P-R. 2019. Infections caused by carbapenem-resistant *Enterobacteriaceae*: an update on therapeutic options. Front Microbiol 10:80. https://doi.org/10.3389/fmicb.2019.00080
12. Qureshi ZA, Paterson DL, Potoski BA, Kilayko MC, Sandovsky G, Sordillo E, Polsky B, Adams-Haduch JM, Doi Y. 2012. Treatment outcome of bacteremia due to KPC-producing *Klebsiella pneumoniae*: superiority of combination antimicrobial regimens. Antimicrob Agents Chemother 56:2108–2113. https://doi.org/10.1128/AAC.06268-11
13. Tsuji BT, Pogue JM, Zavascki AP, Paul M, Daikos GL, Forrest A, Giacobbe DR, Viscoli C, Giamarellou H, Karaiskos I, Kaye D, Mouton JW, Tam VH, Thamlikitkul V, Wunderink RG, Li J, Nation RL, Kaye KS. 2019. International consensus guidelines for the optimal use of the polymyxins: endorsed by the American College of Clinical Pharmacy (ACCP), European Society of Clinical Microbiology and Infectious Diseases (ESCMID), Infectious Diseases Society of America (IDSA), International Society for Anti-infective Pharmacology (ISAP), Society of Critical Care Medicine (SCCM), and Society of Infectious Diseases Pharmacists (SIDP). Pharmacotherapy 39:10–39. https://doi.org/10.1002/phar.2209
14. Kaye KS, Marchaim D, Thamlikitkul V, Carmeli Y, Chiu C-H, Daikos G, Dhar S, Durante-Mangoni E, Gikas A, Kotanidou A, et al. 2023. Colistin monotherapy versus combination therapy for carbapenem-resistant organisms. NEJM Evid 2:EVIDoa2200131. https://doi.org/10.1056/evidoa2200131
15. Paul M, Daikos GL, Durante-Mangoni E, Yahav D, Carmeli Y, Benattar YD, Skiada A, Andini R, Eliakim-Raz N, Nutman A, et al. 2018. Colistin alone versus colistin plus meropenem for treatment of severe infections caused by carbapenem-resistant Gram-negative bacteria: an open-label, randomised controlled trial. Lancet Infect Dis 18:391–400. https://doi.org/10.1016/S1473-3099(18)30099-9
16. Ribeiro AC da S, Chikhani YC dos SA, Valiatti TB, Valêncio A, Kurihara MNL, Santos FF, Minarini LA da R, Gales AC. 2023. *In vitro* and *in vivo* synergism of fosfomycin in combination with meropenem or polymyxin B against KPC-2-producing *Klebsiella pneumoniae* clinical isolates. Antibiotics (Basel) 12:237. https://doi.org/10.3390/antibiotics12020237
17. Hanafin PO, Kwa A, Zavascki AP, Sandri AM, Scheetz MH, Kubin CJ, Shah J, Cherng BPZ, Yin MT, Wang J, Wang L, Calfee DP, Bolon M, Pogue JM, Purcell AW, Nation RL, Li J, Kaye KS, Rao GG. 2023. A population pharmacokinetic model of polymyxin B based on prospective clinical data to inform dosing in hospitalized patients. Clin Microbiol Infect 29:1174–1181. https://doi.org/10.1016/j.cmi.2023.05.018
18. Wilhelm CM, Antochevis LC, Magagnin CM, Arns B, Vieceli T, Pereira DC, Lutz L, de Souza ÂC, Dos Santos JN, Guerra RR, Medeiros GS, Santoro L, Falci DR, Rigatto MH, Barth AL, Martins AF, Zavascki AP. 2024. Susceptibility evaluation of novel beta-lactam/beta-lactamase inhibitor combinations against carbapenem-resistant *Klebsiella pneumoniae* from bloodstream infections in hospitalized patients in Brazil. J Glob Antimicrob Resist 38:247–251. https://doi.org/10.1016/j.jgar.2024.06.007
19. Papp-Wallace KM, Mack AR, Taracila MA, Bonomo RA. 2020. Resistance to novel β-lactam-β-lactamase inhibitor combinations: the "Price of progress". Infect Dis Clin North Am 34:773–819. https://doi.org/10.1016/j.idc.2020.05.001
20. Sun D, Rubio-Aparicio D, Nelson K, Dudley MN, Lomovskaya O. 2017. Meropenem-vaborbactam resistance selection, resistance prevention, and molecular mechanisms in mutants of KPC-producing *Klebsiella pneumoniae*. Antimicrob Agents Chemother 61:e01694-17. https://doi.org/10.1128/AAC.01694-17
21. Humphries RM, Yang S, Hemarajata P, Ward KW, Hindler JA, Miller SA, Gregson A. 2015. First report of ceftazidime-avibactam resistance in a KPC-3-expressing *Klebsiella pneumoniae* isolate. Antimicrob Agents Chemother 59:6605–6607. https://doi.org/10.1128/AAC.01165-15
22. Abdul Rahim N, Cheah S-E, Johnson MD, Yu H, Sidjabat HE, Boyce J, Butler MS, Cooper MA, Fu J, Paterson DL, Nation RL, Bergen PJ, Velkov T, Li J. 2015. Synergistic killing of NDM-producing MDR *Klebsiella pneumoniae* by two "old" antibiotics-polymyxin B and chloramphenicol. J Antimicrob Chemother 70:2589–2597. https://doi.org/10.1093/jac/dkv135
23. Garcia E, Diep JK, Sharma R, Hanafin PO, Abboud CS, Kaye KS, Li J, Velkov T, Rao GG. 2021. Evaluation strategies for triple-drug combinations against carbapenemase-producing *Klebsiella pneumoniae* in an *in vitro* hollow-fiber infection model. Clin Pharmacol Ther 109:1074–1080. https://doi.org/10.1002/cpt.2197
24. Wistrand-Yuen P, Olsson A, Skarp K-P, Friberg LE, Nielsen EI, Lagerbäck P, Tängdén T. 2020. Evaluation of polymyxin B in combination with 13 other antibiotics against carbapenemase-producing *Klebsiella pneumoniae* in time-lapse microscopy and time-kill experiments. Clin Microbiol Infect 26:1214–1221. https://doi.org/10.1016/j.cmi.2020.03.007
25. Daikos GL, Tsaousi S, Tzouvelekis LS, Anyfantis I, Psichogiou M, Argyropoulou A, Stefanou I, Sypsa V, Miriagou V, Nepka M, Georgiadou S, Markogiannakis A, Goukos D, Skoutelis A. 2014. Carbapenemase-producing *Klebsiella pneumoniae* bloodstream infections: lowering mortality by antibiotic combination schemes and the role of carbapenems. Antimicrob Agents Chemother 58:2322–2328. https://doi.org/10.1128/AAC.02166-13
26. Michalopoulos A, Virtzili S, Rafailidis P, Chalevelakis G, Damala M, Falagas ME. 2010. Intravenous fosfomycin for the treatment of nosocomial infections caused by carbapenem-resistant *Klebsiella pneumoniae* in critically ill patients: a prospective evaluation. Clin Microbiol Infect 16:184–186. https://doi.org/10.1111/j.1469-0691.2009.02921.x
27. Sharma R, Patel S, Abboud C, Diep J, Ly NS, Pogue JM, Kaye KS, Li J, Rao GG. 2017. Polymyxin B in combination with meropenem against carbapenemase-producing *Klebsiella pneumoniae*: pharmacodynamics and morphological changes. Int J Antimicrob Agents 49:224–232. https://doi.org/10.1016/j.ijantimicag.2016.10.025
28. Golla VK, Sans-Serramitjana E, Pothula KR, Benier L, Bafna JA, Winterhalter M, Kleinekathöfer U. 2019. Fosfomycin permeation through the outer membrane porin OmpF. Biophys J 116:258–269. https://doi.org/10.1016/j.bpj.2018.12.002
29. Kaye KS, Rice LB, Dane AL, Stus V, Sagan O, Fedosiuk E, Das AF, Skarinsky D, Eckburg PB, Ellis-Grosse EJ. 2019. Fosfomycin for injection (ZTI-01) versus piperacillin-tazobactam for the treatment of complicated urinary tract infection including acute pyelonephritis: ZEUS, a phase 2/3 randomized trial. Clin Infect Dis 69:2045–2056. https://doi.org/10.1093/cid/ciz181
30. Trimble MJ, Mlynárčik P, Kolář M, Hancock REW. 2016. Polymyxin: alternative mechanisms of action and resistance. Cold Spring Harb Perspect Med 6:a025288. https://doi.org/10.1101/cshperspect.a025288
31. Poirel L, Jayol A, Bontron S, Villegas M-V, Ozdamar M, Türkoglu S, Nordmann P. 2015. The *mgrB* gene as a key target for acquired resistance to colistin in *Klebsiella pneumoniae*. J Antimicrob Chemother 70:75–80. https://doi.org/10.1093/jac/dku323
32. Fedrigo NH, Shinohara DR, Mazucheli J, Nishiyama SAB, Carrara-Marroni FE, Martins FS, Zhu P, Yu M, Sy SKB, Tognim MCB. 2021. Pharmacodynamic evaluation of suppression of *in vitro* resistance in *Acinetobacter baumannii* strains using polymyxin B-based combination therapy. Sci Rep 11:11339. https://doi.org/10.1038/s41598-021-90709-2
33. MacNair CR, Stokes JM, Carfrae LA, Fiebig-Comyn AA, Coombes BK, Mulvey MR, Brown ED. 2018. Overcoming *mcr-1* mediated colistin

resistance with colistin in combination with other antibiotics. Nat Commun 9:458. https://doi.org/10.1038/s41467-018-02875-z
34. Han L, Xu F-M, Zhang X-S, Zhang C-H, Dai Y, Zhou Z-Y, Wang Y-X, Chen F, Shi D-W, Lin G-Y, Yu X-B. 2022. Trough polymyxin B plasma concentration is an independent risk factor for its nephrotoxicity. Br J Clin Pharmacol 88:1202–1210. https://doi.org/10.1111/bcp.15061
35. Imani S, Buscher H, Marriott D, Gentili S, Sandaradura I. 2017. Too much of a good thing: a retrospective study of β-lactam concentration-toxicity relationships. J Antimicrob Chemother 72:2891–2897. https://doi.org/10.1093/jac/dkx209
36. Bassetti M, Peghin M, Vena A, Giacobbe DR. 2019. Treatment of infections due to MDR Gram-negative bacteria. Front Med 6:74. https://doi.org/10.3389/fmed.2019.00074
37. Karaiskos I, Lagou S, Pontikis K, Rapti V, Poulakou G. 2019. The "Old" and the "New" antibiotics for MDR Gram-negative pathogens: for whom, when, and how. Front Public Health 7:151. https://doi.org/10.3389/fpubh.2019.00151
38. Nielsen EI, Khan DD, Cao S, Lustig U, Hughes D, Andersson DI, Friberg LE. 2017. Can a pharmacokinetic/pharmacodynamic (PKPD) model be predictive across bacterial densities and strains? External evaluation of a PKPD model describing longitudinal *in vitro* data. J Antimicrob Chemother 72:3108–3116. https://doi.org/10.1093/jac/dkx269
39. Aranzana-Climent V, van Os W, Nutman A, Lellouche J, Dishon-Benattar Y, Rakovitsky N, Daikos GL, Skiada A, Pavleas I, Durante-Mangoni E, Theuretzbacher U, Paul M, Carmeli Y, Friberg LE. 2024. Integration of individual preclinical and clinical anti-infective PKPD data to predict clinical study outcomes. Clin Transl Sci 17:e13870. https://doi.org/10.1111/cts.13870
40. Andrews JM, Baquero F, Beltran JM, Canton E, Crokaert F, Gobernado M, Gomez-Ius R, Loza E, Navarro M, Olay T. 1983. International collaborative study on standardization of bacterial sensitivity to fosfomycin. J Antimicrob Chemother 12:357–361. https://doi.org/10.1093/jac/12.4.357
41. CLSI. 2024. M100 Ed34. Performance standards for antimicrobial susceptibility testing. 34th ed. Clinical & Laboratory Standards Institute.
42. EUCAST. 2025. Clinical Breakpoint Tables v. 15.0, valid from 2025-01-01. Available from: https://www.eucast.org/fileadmin/src/media/PDFs/EUCAST_files/Breakpoint_tables/v_15.0_Breakpoint_Tables.pdf. Retrieved 26 Sep 2025.
43. Monteiro J, Widen RH, Pignatari ACC, Kubasek C, Silbert S. 2012. Rapid detection of carbapenemase genes by multiplex real-time PCR. J Antimicrob Chemother 67:906–909. https://doi.org/10.1093/jac/dkr563
44. Kaczmarek FM, Dib-Hajj F, Shang W, Gootz TD. 2006. High-level carbapenem resistance in a *Klebsiella pneumoniae* clinical isolate is due to the combination of bla_{ACT-1} β-lactamase production, porin OmpK35/36 insertional inactivation, and down-regulation of the phosphate transport porin phoe. Antimicrob Agents Chemother 50:3396–3406. https://doi.org/10.1128/AAC.00285-06
45. Diep JK, Jacobs DM, Sharma R, Covelli J, Bowers DR, Russo TA, Rao GG. 2017. Polymyxin B in combination with rifampin and meropenem against polymyxin B-resistant KPC-producing *Klebsiella pneumoniae*. Antimicrob Agents Chemother 61:e02121-16. https://doi.org/10.1128/AAC.02121-16
46. Ehmann L, Zoller M, Minichmayr IK, Scharf C, Huisinga W, Zander J, Kloft C. 2019. Development of a dosing algorithm for meropenem in critically ill patients based on a population pharmacokinetic/pharmacodynamic analysis. Int J Antimicrob Agents 54:309–317. https://doi.org/10.1016/j.ijantimicag.2019.06.016
47. Wangchinda W, Pogue JM, Thamlikitkul V, Leelawattanachai P, Koomanachai P, Pai MP. 2024. Population pharmacokinetic/pharmacodynamic target attainment analysis of IV fosfomycin for the treatment of MDR Gram-negative bacterial infections. J Antimicrob Chemother 79:1372–1379. https://doi.org/10.1093/jac/dkae111
48. Luterbach CL, Qiu H, Hanafin PO, Sharma R, Piscitelli J, Lin F-C, Ilomaki J, Cober E, Salata RA, Kalayjian RC, Watkins RR, Doi Y, Kaye KS, Nation RL, Bonomo RA, Landersdorfer CB, van Duin D, Rao GG. 2022. A systems-based analysis of mono- and combination therapy for carbapenem-resistant *Klebsiella pneumoniae* bloodstream infections. Antimicrob Agents Chemother 66:e00591. https://doi.org/10.1128/aac.00591-22
49. Landersdorfer CB, Ly NS, Xu H, Tsuji BT, Bulitta JB. 2013. Quantifying subpopulation synergy for antibiotic combinations via mechanism-based modeling and a sequential dosing design. Antimicrob Agents Chemother 57:2343–2351. https://doi.org/10.1128/AAC.00092-13
50. Bulitta JB, Ly NS, Yang JC, Forrest A, Jusko WJ, Tsuji BT. 2009. Development and qualification of a pharmacodynamic model for the pronounced inoculum effect of ceftazidime against *Pseudomonas aeruginosa*. Antimicrob Agents Chemother 53:46–56. https://doi.org/10.1128/AAC.00489-08
51. Beal SL. 2001. Ways to fit a PK model with some data below the quantification limit. J Pharmacokinet Pharmacodyn 28:481–504. https://doi.org/10.1023/a:1012299115260
52. Bulitta JB, Bingölbali A, Shin BS, Landersdorfer CB. 2011. Development of a new pre- and post-processing tool (SADAPT-TRAN) for nonlinear mixed-effects modeling in S-ADAPT. AAPS J 13:201–211. https://doi.org/10.1208/s12248-011-9257-x